

PARTIAL DIFFERENTIAL EQUATIONS BASED IMAGE ANALYSIS WITH APPLICATIONS IN SAR With MEDICAL IMAGES

Murthoty Satheesh Babu, Research Scholar, Department of Electronics and communication Engineering, Monad University, Hapur, U.P.

Dr.Jaidev Sharma, Associate Professor, Supervisor, Department of Electronics and communication Engineering, Monad University, Hapur, U.P.

Abstract:

The intersection of partial differential equation analysis and applications to computer vision and image processing is the subject of this dissertation. For lowering the "staircasing" effect shown in the findings of the robust anisotropic diffusion model published by Black et al. as well as the traditional anisotropic diffusion model offered by Perona and Malik, two robust heterogeneity scales are recommended in the first half of this thesis. The recommended scales were created using good statistical change-point detection theory and reliable L-estimators. In order to correctly estimate the noise level for a noisy image, neither the Perona-Malik model nor the robust model are successful. As a result, the impact of staircasing grows as more objects are added. According to experimental results, the recommended heterogeneity scales might significantly eliminate the aforementioned abnormalities in the trusted anisotropic diffusion model. To minimize speckle noise, which is mostly prevalent in SAR and medical ultrasound images, a robust diffusion function is created using the notion of a robust M-estimation technique and a multiplicative noise model. Proposed robust heterogeneity scales are coupled with a newly developed diffusion function to reduce multiplicative noise. In tests, the performance of the novel speckle-reducing method is evaluated using test photographs as well as real SAR and USG images. The experimental results unmistakably demonstrate that the proposed approach outperforms the existing speckle reduction strategies described in the literature. The thesis's closing portion discusses the segmentation of brain MR images using PDEs. The cerebral cortex has a complex anatomical structure, making parametric mapping

of the cortex in MR images of the brain challenging. The generalized gradient vector flow (GGVF) model published by Xu and Prince and the conventional active contour model (often referred to as a snake) proposed by Kass, Witkin, and Terzopoulos (KWT) may both be used to partially achieve this aim. Unfortunately, the Partial Volume Effect (PVE) prevents both parametric models from resolving the deep sulcal folds of the cerebral cortex. This thesis proposes a new model that accomplishes this task utilizing prior understanding of the structure of the brain. To overcome the obstacles, a specially customized internal force field is developed based on the local curvature of the growing snake. A powerful external force field is also used to drag the snake into the deep sulcal folds of the cerebral cortex. It is possible to reach the deep concavities of the sulcus utilizing a hybrid model that incorporates the above-mentioned internal and external force fields. This hybrid model selects either the classic snake or the GGVF snake, depending on the requirement, to efficiently access the deep sulcal folds of the cerebral cortex.

1 Introduction

Robotic vision, sometimes referred to as machine vision or computer vision, is the automatic perception of visual information produced through careful image content processing. The development of appropriate mathematical models that reformulate the concept of the human perception problem in terms of a sound mathematical theory is required in situations like this. The development of such models that can imitate human vision is still a long way off. Our broad understanding of how the world works involves an understanding of pictures, which requires prior experience. This previous experience impacts our opinions on which elements of the

picture should be given greater attention.

The greatest degree of human perception of a situation is something that we now only have a very limited understanding of. What is known is that the brain allocates high information value to vertices, linear structures, and edges and divides the portions of the image with comparable qualities into separate areas [Res89]. Since texture has such an impact on human perception, it is even possible to segment images only using texture [DMM08]. It is also very size-adaptable, able to recognize structure within a type while categorizing whole regions of a picture as a single category (forest, throng, etc.).

The study of image processing fills the knowledge gap between machine vision

and high-level human cognition of the scene by bridging the physical viewpoint of the environment that produced the image. Image processing aims to analyze a picture, whether it be analog or digital, in order to extract its features. These characteristics are necessary for higher level machine perception. In image processing, segmentation and denoising/restoration are both essential steps. The present thesis focuses on partial differential equations (PDEs)-based methods for image restoration and segmentation. Partial differential equation-based image processing is one of the theoretically most sound methods, and it has spawned a brand-new field of computer vision. Researchers have published hundreds of articles over the last few decades, and PDE-based methods are often utilized at conferences and seminars.

Since the beginning of the 19th century, partial differential equations have been the main mathematical tools for expressing physical models (laws) of both classical and modern physics. Examples of partial differential equations include Maxwell's equations in electromagnetic theory, Hamilton-Jacobi equations in classical mechanics, Schrödinger's equation in quantum mechanics, etc. PDEs have been used to depict mathematical models in many

fields, including biology and economics, for around 50 years. Image processing PDE applications are a very recent development. Koenderink [Koe84] was the first to demonstrate the connection between PDE and the notion of Gaussian scale space in image processing. He noticed that by convoluting the image with a Gaussian at some scale (variance), the heat equation could be solved using the image as a starting datum. Formally, this may be stated as follows: If the symbol u_0 denotes the original image, the "scale space" analysis associated with u_0 is created by solving the system.

2 Literature survey

By selecting a tiny kernel of pixels and swiping them over the whole picture, spatial domain filtering techniques directly affect the image. This method works better for enhancing the contrast of the picture and defining its details. Additionally, this method's drawback is that it processes local information rather than frequencies while ignoring the borders. In order to estimate the radar reflectivity from the speckled picture, the topic is handled from the standpoint of SAR despeckling (Touzi 2002). According to estimation theory, improved parameter estimate is only possible if the process is ergodic,

stationary, and monitored at regular intervals. The sample is gathered at a limited interval, and the sample average is approximated using ergodicity and stationary distribution, respectively. Consequently, depending on the scene, the speckle filtering may be classified as either a stationary or non-stationary function. In order to determine the noise ratio as a constant for the whole picture and compute it just once, the majority of speckle filtering techniques require that the speckle noises are stationary and multiplicative in nature. Following are the several categories of filters that can handle both stationary and non-stationary speckle noises:

The assumption made by SMSM filters like Lee's (Lee 1980), Frost's (Frost et al. 1982), and Kuan's (Kuan et al. 1985) is that the speckle remains stationary across the whole picture. The multiplicative speckle model serves as the foundation for these filters. Here, the despeckling is carried out non-homomorphically, that is, in the original domain rather than after log transformation. Filters that use a multiplicative speckle model (NSMSM filters) presumptively presume that speckle is not locally stable inside the kernel. The intensity speckle mean is non-stationary because these filters, like

the MAP Gaussian filter (Kuan et al. 1987), are based on the product model.

Lee (1980) suggested a spatial domain filtering method based on calculating the sliding kernel's local statistics. For each kernel, the Minimum Mean Square Error (MMSE) is determined in order to choose the best weight function for kernel updation. Even though the Lee filter offers higher speckle suppression, its lack of adaptive properties causes it to oversmooth the picture. Frost filter is an adaptively weighted average filter (Frost et al. 1982). Here, the ideal MMSE for despeckling is estimated. It uses MMSE in homogenous regions and each kernel's local mean and variance to achieve adaptiveness. The Frost filter has the ability to remove specks while keeping the image's characteristics. In diverse places, however, the lines between them are hazy. The frost filter can produce superior Peak Signal to Noise Ratio (PSNR) and Edge Preserving Index (EPI), but since it only eliminates a tiny quantity of speckles, it has no effect on the aesthetic quality of the photos. As a result, the frost filter is underutilized despite its suitability for modifying applications based on low speckled images (Mascarenhas 1997). Mean and Median filters are typical low pass filters used for denoising because

of their special smoothing and smearing capabilities. Both filters lack adaptiveness and are inappropriate for photos with substantial noise variation. Therefore, the filtering process includes adaptive filters. In order to convert the Lee filter into an adaptive filter, Kuan et al. (1985) estimated the nonstationary mean and nonstationary variance. Kuan filter demonstrated its suitability for many noise kinds and its lack of need on previous information of the picture. The Kuan filter's drawback is that it oversmooths the textures and edges (Ali et al. 2007, for example).

Kalman filter-based despeckling filter was suggested by Subrahmanyam et al. (2008). Although the speckle is a multiplicative noise, it is appropriate for additive noise in nature. The Importance Sampling Unscented Kalman Filter (ISUKF) is a hybrid Kalman filter that uses a Markov conditional PDF to estimate the first two moments by sampling. The sigma points are utilized to define the noise characteristics, and the Markov PDF prevents over-smoothing of borders and homogenous regions. Anisotropic diffusion approach based on an adaptable kernel was suggested by Liu et al. in 2009, with the size and orientation of the kernel being flexible. While stabilizing the other aspects of the picture, the anisotropic

diffusion approach is utilized to suppress the speckle noise using the local statistics derived for the kernel. The diffusion approach maintains the algorithm more consistent while the adaptive window size lessens the impact of oversmoothing on the boundaries. But this filtering might harm the edges of the discontinued products.

3 Methodology:

Typically, modeling PDE-based picture restoration employs two strategies. In contrast to weak or variational formulations where an appropriate energy functional (in terms of an integral) is constructed for optimization and the restored pictures are provided by the steady-state of this process, strong formulations directly define the PDE from the hypothesis. In certain instances, the energy term that has to be solved for restoration is used to generate Euler-Lagrange equations. For the purpose of developing models for image processing, both methods are equally valid.

Classical Nonlinear Models:

This section aims to provide some of the traditional PDE-based picture restoration techniques. We'll go through the specific mathematical characteristics of these evolution equations as well as the numerous theoretical and practical ramifications that these models have.

These models may generally be formalized as follows:

$$\begin{cases} \frac{\partial u(t, x)}{\partial t} + F(x, u(t, x), \nabla u(t, x), \nabla^2 u(t, x)) = 0 \text{ in } \Omega \\ \frac{\partial u(t, x)}{\partial \nu} = 0 \text{ in } \partial\Omega \\ u(0, x) = u_0(x) \end{cases}$$

$x \in \mathbb{R}^p, p > 0$, for a 2D picture with $p=2$, u_0 is the original (noisy) image, $u(t, x)$ is the restored (smoothed to a finer scale) image at time $t > 0$, and ν is the outward drawn normal on boundary. The gradient is denoted by $\nabla u(t, x)$, while the Hessian is denoted by $\nabla^2 u(t, x)$. In order to generate the family of subsequent functions of structurally simpler pictures $u(t, x), t > 0$, equation (2.1) must first be solved beginning from the initial image $u_0(x)$. Because finer visual structures are lost as time t increases, it is referred to as the scale. A important condition for $u(t, x)$ evolution is that no new structures (artefacts) are formed during the evolution process and that the coarse-scale representations should consist of simplifications of the equivalent structures at finer scales. Different PDE models are created as a result of these needs and a few more.

Linear Diffusion :

The first method [Koe84], [AGLM93] for encoding an $u_0(x)$ picture at various scales is to regard the image as the starting value of the homogenous linear diffusion equation: where denotes

Laplacian, i.e. Δu . Equation depicts a straightforward second order hyperbolic PDE with the diffusion coefficient considered to be constant at 1. The scaled copies of the original picture are given by the equation's solution for $t > 0$ as

$$\begin{cases} \frac{\partial u(t, x)}{\partial t} - \Delta u(t, x) = 0 \text{ in } \Omega \\ u(0, x) = u_0 \end{cases}$$

$$u(t, x) = (K_{\sqrt{2t}} * u)(x) = \int_{\mathbb{R}^2} (u(y) K_{\sqrt{2t}}(x - y)) dy$$

$$K_{\sigma}(x) = \frac{1}{2\pi\sigma^2} e^{-\left(\frac{x^T x}{2\sigma^2}\right)}$$

where K represents a 2-dimensional Gaussian with a standard deviation of $\sqrt{2t}$. Observe how Equation extends the scope of u_0 to \mathbb{R}^2 by repeating the picture around the border. If $|u_0| dx$ is added, it may be claimed that $u_0 \in L^1(\mathbb{R}^2)$. The result of solving an equation on an image is thus the same as that of a Gaussian convolution.

4 Experiment & Evaluation

Consider a parametric statistical model $(\Omega, \mathcal{P}; \theta)$, where Ω denotes the sample space, the event-field, and \mathcal{P} the probability measure from the family \mathcal{P} : of probability distributions. Usually, the set of unknown parameters, θ , is denoted by $\mathbb{R}^p, p > 0$.

The result of each observation, x_i , relies on the "true value" of the unknown

parameter and some i.i.d. noise, e_i , according to the most basic statistical model that is often assumed for location estimation. The assumption that noise is additive in most straightforward situations is $x_i = \theta + e_i$.

The location model is what is used in this. The basic objective is to identify an estimate that depends on the observations x_1, x_2, \dots, x_n with a high degree of probability. It is agreed that the observations represent the realization of some random variable X . Additionally, it is expected that $T(x_1, x_2, \dots, x_n)$ is a shift/scale equivariant (linear) functional of the observations. Mean square estimate (MSE) is a popular method of approximating :

$$\text{MSE}(\theta) = E(\theta - \hat{\theta})^2$$

Traditional statistical techniques would presuppose "well behaved" data from a population with distribution F , as well as the fact that F is a member of a well defined family of parametric distributions. Since processes based on the normality assumption often have a straightforward algebraic structure, it is assumed that this distribution F is normal in the majority of circumstances. For instance, the mean is the best estimate if F is perfectly normal and maximum likelihood estimation (MLE) is used as the estimation method. Traditional optimal estimate, however,

struggles to provide adequate results when data is polluted by outliers because of the effect of contaminants. Skewed (asymmetric) or longer-tailed distributions are only two examples of how the divergence from the normal distribution might appear. A popular technique for representing "contaminated" distributions was developed by Tukey [Tuk60] and is given by the formula $F = H + (1 - \alpha)G$, where $GN(\mu, \sigma^2)$ and H are any other distributions, possibly another normal distribution with a different mean and larger variance, and α denotes a small portion of the mixture of two distributions.

The diffusion of the Lena picture by Perona_Malik with a static scale of 65 is shown in Fig. The second row demonstrates how the picture becomes noticeably blurry and loses its edges after 60 rounds. The identical picture is shown in Fig. 3.4 after 120 iterations with matching Canny edges [Can86], [Der87]. Now that practically all of the edges have been lost, the picture is quite blurry. This occurred as a result of both the manual setting of the heterogeneity scale and the non-robust nature of the edge-stopping function of the Perona-Malik diffusion process.

The outcome of robust diffusion utilizing Tukey's bi-weight function and

MAD as a measure of heterogeneity is shown in Fig. The findings make it quite evident how much the preservation of edges and other heterogeneous features has dramatically improved. As opposed to Fig, which demonstrates how using a robust functional may significantly enhance the final diffusion process.



Figure 4.1 (a) The original Lena image; (b) Canny edge of the original image; (c) P-M diffused image after 60 iterations with static scale $\lambda=65$; (d) Canny edge of P-M diffused image.

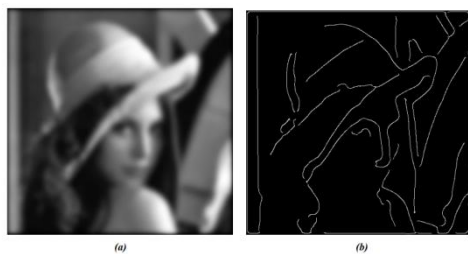


Figure 4.2 (a) P-M diffused Lena image after 120 iterations with static scale $\lambda=65$; (b) Canny edge of P-M diffused image.

However, even using a strong redescending function to smooth the pictures, as shown in Fig, the staircasing effect still cannot be eliminated. The staircasing effect in the picture may be seen more clearly if you look at it closely. An enlarged portion of the face around the lips and nose is shown in Fig. 3.6(a) and (b), where this effect becomes quite obvious. Naturally, the issue of what may have caused this oddity emerges. And can the staircasing effect be eliminated without looking for another reliable diffusion function?

The selection of MAD as the heterogeneity scale in Black and Sapiro's technique may provide a crucial hint. Despite its resilience, MAD adopts a symmetric perspective on dispersion since it assigns equal weight to positive and negative departures from a central value (the median), which does not appear to be a natural strategy for asymmetric distributions. Of course, there is nothing to prevent us from employing the MAD for highly skewed distributions, although doing so may be fairly ineffective and unnatural, as Rousseeuw et al [RC93] noted. As a consequence, MAD produces artifacts during iterations when there is a lot of noise and is unable to choose the appropriate scale.

5 conclusion

Medical imaging techniques including CT, SPECT, PET, MRI, fMRI, etc., as well as one of the many microscopy platforms, have grown significantly during the last three decades [Sue09]. These technologies have significantly changed how many illnesses are diagnosed and provide a non-invasive technique to see within the human body. The usual patient diagnostic procedure now includes three dimensional volumetric viewing of CT and MRI data of the spine, internal organs, and brain. Every day, pathologists, radiologists, and nuclear medicine specialists create and scan enormous amounts of medical picture data for diagnostic purposes in hospitals. This has led to the need for automated internal organ or pathology identification. The development of autonomous diagnosis in medical pictures is undoubtedly the most notable breakthrough, and it calls for advancement and innovation in all areas of image processing methods.

Enhancement, segmentation, and feature extraction are the first three main phases in image processing. In analyzing the individual biological or medicinal items, picture segmentation is a crucial step. Today, segmented pictures are often employed for a wide range of purposes, including diagnosis, treatment

planning, disease localization, anatomical structure analysis, and computer-assisted surgery. However, owing to both the diversity of item forms and the fluctuation in picture quality, segmenting medical images remains a challenging process. Particularly, noise and sampling artifacts often taint biological pictures, which may provide significant challenges when using strict methodologies.

6 References

- [1] R. Achanta, F. Estrada, P. Wils, and S. Süsstrunk, "Salient region detection and segmentation," in International conference on computer vision systems. Springer, 2008, pp. 66–75.
- [2] R. K. Aggarwal and M. Dave, "Filterbank optimization for robust asr using ga and pso," International Journal of Speech Technology, vol. 15, no. 2, pp. 191–201, 2012.
- [3] S. Agrawal, R. Panda, S. Bhuyan, and B. K. Panigrahi, "Tsallis entropy based optimal multilevel thresholding using cuckoo search algorithm," Swarm and Evolutionary Computation, vol. 11, pp. 16–30, 2013.
- [4] B. Akay, "A study on particle swarm optimization and artificial bee colony algorithms for multilevel thresholding," Applied Soft Computing, vol. 13, no. 6, pp. 3066–3091, 2013.

- [5] A. Al-Ajlan and A. El-Zaart, "Image segmentation using minimum cross-entropy thresholding," in *Systems, Man and Cybernetics*, 2009. SMC 2009. IEEE International Conference on. IEEE, 2009, pp. 1776–1781.
- [6] M. N. Alam, "Particle swarm optimization: Algorithm and its codes in matlab," 2016.
- [7] M. Ali, C. W. Ahn, and M. Pant, "Multi-level image thresholding by synergetic differential evolution," *Applied Soft Computing*, vol. 17, pp. 1–11, 2014.
- [8] A. Z. Arifin and A. Asano, "Image segmentation by histogram thresholding using hierarchical cluster analysis," *Pattern Recognition Letters*, vol. 27, no. 13, pp.1515–1521, 2006.
- [9] S. Arora, J. Acharya, A. Verma, and P. K. Panigrahi, "Multilevel thresholding for image segmentation through a fast statistical recursive algorithm," *Pattern Recognition Letters*, vol. 29, no. 2, pp. 119–125, 2008.
- [10] H. V. H. Ayala, F. M. dos Santos, V. C. Mariani, and L. dos Santos Coelho, "Image thresholding segmentation based on a novel beta differential evolution approach," *Expert Systems with Applications*, vol. 42, no. 4, pp. 2136–2142, 2015.
- [11] L. Barghout, "Vision. global conceptual context changes local contrast processing (ph. d. dissertation 2003). updated to include computer vision techniques. scholars' press," ISBN 978-3-639-70962-9, Tech. Rep., 2014.
- [12] "Visual taxometric approach to image segmentation using fuzzy-spatial taxon cut yields contextually relevant regions," in *International Conference on Information Processing and Management of Uncertainty in Knowledge-Based Systems*. Springer, 2014, pp. 163–173.
- [13] L. Barghout and L. Lee, "Perceptual information processing system," Mar. 25 2004, uS Patent App. 10/618,543.
- [14] L. Barghout and J. Sheynin, "Real-world scene perception and perceptual organization: Lessons from computer vision," *Journal of Vision*, vol. 13, no. 9, pp. 709–709, 2013.
- [15] S. Baskar, A. Alphones, P. Suganthan, and J. Liang, "Design of yagi-uda antennas using comprehensive learning particle swarm optimisation," *IEE Proceedings Microwaves, Antennas and Propagation*, vol. 152, no. 5, pp. 340–346, 2005.
- [16] K. J. Batenburg and J. Sijbers, "Adaptive thresholding of tomograms by projection distance minimization," *Pattern Recognition*, vol. 42, no. 10, pp. 2297–2305, 2009.

- [17]“Optimal threshold selection for tomogram segmentation by projection distance minimization,” IEEE Transactions on Medical Imaging, vol. 28, no. 5, p.676, 2009.
- [18] S. Beevi, M. S. Nair, and G. Bindu, “Automatic segmentation of cell nuclei using krill herd optimization based multi-thresholding and localized active contour model,” Biocybernetics and Biomedical Engineering, vol. 36, no. 4, pp. 584–596,2016.
- [19] A. K. Bhandari, A. Kumar, and G. K. Singh, “Modified artificial bee colony based computationally efficient multilevel thresholding for satellite image segmentation using kapur’s, otsu and tsallis functions,” Expert Systems with Applications, vol. 42, no. 3, pp. 1573–1601, 2015.
- [20]“Tsallis entropy based multilevel thresholding for colored satellite image segmentation using evolutionary algorithms,” Expert Systems with Applications, vol. 42, no. 22, pp. 8707–8730, 2015.
- [21] A. K. Bhandari, V. K. Singh, A. Kumar, and G. K. Singh, “Cuckoo search algorithm and wind driven optimization based study of satellite image segmentation for multilevel thresholding using kapur’s entropy,” Expert Systems with Applications, vol. 41, no. 7, pp. 3538–3560, 2014.